1 Introduction

The land-ocean aquatic continuum is commonly defined as the interface, or transition zone, between terrestrial ecosystems and the open ocean (Billen et al., 1991; Mackenzie et al., 2012, Rabouille et al., 2001, Regnier et al., submitted). This continuum includes inland waters, estuaries and coastal waters (Billen et al. 1991, Crossland, 2005, Liu, 2010), a succession of biogeochemically and physically active systems that not only process large quantities of carbon and nutrients during their natural transit from upland soils to the open ocean (Arndt et al., 2007 & 2009, Laruelle, 2009, Mackenzie et al., 2005, Nixon et al., 1996, Regnier and Steefel, 1999, Vanderborght et al. 2002 & 2007), but also exchange vertically significant amounts of greenhouse gases with the atmosphere (Cole et al., 2007, Laruelle et al., 2010, Tranvik et al., 2009). Although the land-ocean aquatic continuum is acknowledged to play a significant role in global biogeochemical cycles (Gattuso et al. 1998, Mackenzie et al., 1998, Mantoura et al., 1991), the quantitative contribution of fresh water, estuaries and continental shelves to carbon and nutrient budgets remains entailed with large uncertainties, reflecting primarily the limited availability of field data and the lack of robust upscaling approaches (Regnier et al., submitted).

Over the past few years, a growing number of environmental databases dedicated to inland waters (GLORICH, Hartmann et al., 2011), estuaries (Engle et al., 2007) and the coastal zone have been assembled (LOICZ, Crossland, 2005). Extrapolation of the numerous local measurements in these databases to provide regional and global budgets calls for the segmentation of the aquatic continuum into areas of broadly similar biogeochemical and physical behaviour, based on multiple criteria such as climate, morphology and physical forcings. In addition, the surface area and volume of the resulting segments need to be constrained for budgeting purposes, a task that is more complex that one might actually presume. For instance, the geographical extent of the continental shelf itself (i.e. the extended

perimeter of a continent, usually covered by shallow seas) is still a matter of debate (Borges et al., 2005, Chen et al., 2011, Liu, 2010), partly because there is no common definition of its outer limit. So far, the delineation of the coastal ocean has been constrained using administrative limits (Sherman et al., 1989), the 200 m isobaths (Walsh et al., 1998), the maximum increase in slope of the seabed (Liu, 2010), leading to surface area estimates that differ by up to 20 %. Similar issues arise for the delineation of regional boundaries on land (Meybeck et al., 2006). It has however been shown that a careful segmentation of continental shelf seas into representative units together with a robust, GIS-based estimation of the corresponding surface areas contribute to improved biogeochemical budgets, as exemplified by the revised global air-water CO_2 exchange flux estimated by (Laruelle et al., 2010) for the coastal ocean.

At the global scale, a segmentation that incorporates consistently the aquatic continuum of fresh waters, estuaries and continental shelves remains to be developed. A major difficulty arises because their spatial scales are fundamentally different and may vary regionally. For instance, estuaries exhibit typical length and width scales of 10-100 km and 1-10 km, respectively, and are thus much smaller entities than large scale coastal entities delimited by well established currents such as the Gulf Stream or the California current which flow along continents over thousands of kilometers (Longhurst, 1998). The largest rivers in the world exceed thousands of km in length but require a representation of their river network at resolutions <1 degree for a proper identification of the routing of their main tributaries (Vörösmarty et al., 2002). Moreover, environmental databases gathering monitoring data, climatological forcings and average earth surface properties are available under various forms and at different spatial resolution. Some consists in gridded maps, files or model outputs at 0.5 or 1 degree resolution (World Ocean Atlas, DaSilva et al., 1994, Levitus et al., 1998, GLOBALNEWS, Mayorga et al., 2010, Seitzinger et al., 2005) while others are databases

containing measurements from millions (SOCAT, Pfeil et al., 2012) to thousands (GLORICH) or just several dozen (Lonborg and Alvarez-Salgado, 2012, Laruelle et al., 2010, Seiter et al., 2005) of unevenly distributed sampling points. Thus, for environmental budgeting purposes, a multi-scale approach is required to integrate and combine this variety of databases.

In this study, we present a harmonized multi-scale segmentation for the land-ocean continuum, from the watershed to the outer limit of the continental shelf. It is based on three increasing levels of aggregation and the inter compatibility of these levels not only allows to integrate a wide variety of databases compiled at various spatial resolutions, but also to compare and combine them with one another. The first level, at the finer resolution of 0.5 degrees, is based on the work of Vörösmarty et al., (2000) and resolves the watersheds and river routing. It also attributes an estuarine type to each watershed following the typology of Dürr et al. (2011) which includes small deltas, tidal systems, lagoons and fjords. This spatial resolution allows for a realistic representation of the global river network and is compatible with many global databases (World Ocean Atlas, LOICZ, Buddemeier et al., 2008, Crossland, 2005). This level is also suitable for detailed regional analyses of coastal regions and their corresponding watersheds (Regnier et al., submitted). The second level is built on an updated version of the COSCAT segmentation (Meybeck et al., 2006) which distinguishes different segments of the global coastline based on a combination of terrestrial watershed characteristics and coastal geomorphologic features. It is extended here to include the relevant portions of the adjacent continental shelves. The highest level in the hierarchy is termed MARCATS (for MARgins and CATchment Segmentation) and consists of aggregated COSCAT units according to the main climatological, morphological and oceanographic characteristics of the coastal zone. It is based on the recent synthesis by Liu et al. (2010) and allows for coarser regional analysis and upscaling calculations when datasets are limited. It

nevertheless retains the major physical features of many different coastal regions and identifies a number of widely studied systems such as the main regional seas and some major coastal currents. It can be viewed as an analogue to the coarse segmentation of Takahashi et al. (2009) for the estimation of CO_2 fluxes in the open ocean.

The COSCAT and MARCATS segmentation were used to calculate, for different isobaths, the surface area and volume of each segment of the coastal ocean. The surface areas of watersheds and estuaries are also reported at the same levels. These segmentations can be used in conjunction with biogeochemical databases (e.g. World Ocean Atlas, LOICZ, Hexacoral, GLORICH, SOCAT, and so forth) to establish regional budgets and, eventually, refine global assessments of the carbon and nutrient cycles. This is performed in this study through the form of regionalized estimates of CO_2 fluxes from estuarine systems. The segmentation is also combined with watershed models (e.g. GLOBALNEWS) to constrain, for each region of the world, the amount of freshwater that is routed through the different estuarine types and delivered to a given segment of the coastal ocean. These volumes of freshwater are compared those of the continental shelves they flow into. Although not performed here, the same approach could easily be expanded to terrestrial carbon and nutrient fluxes. Thus the new compiled and homogenized dataset is applicable in a wide range of future investigations of biogeochemical fluxes along the land-ocean continuum which are still largely misrepresented or ignored in current Global Circulation and Earth System Models. The provided GIS-files in the supplement information will allow the community to alter the approach or to refine local settings if needed.

3.5 CO_2 outgassing from estuaries

Globally, estuaries have been identified as net emitters of CO_2 to the atmosphere (Abril and Borges, 2004, Borges 2005, Borges et al., 2005, Cai, 2011, Chen and Borges, 2009, Laruelle et al., 2010). The first set of studies, based on simple upscaling from a few local measurements, provided first-order estimates of CO_2 evasion ranging from 0.4 to 0.6 Pg C yr^{-1} (Abril and Borges, 2004; Borges, 2005; Borges et al., 2005; Chen and Borges, 2009). The more recent work by Laruelle et al., 2010 and Cai, 2011 relying on a more detailed typology of estuarine systems have revised these estimates down to a value of 0.25 ± 0.25 Pg C yr^{-1} (Regnier et al., submitted). Yet, the best available global flux values remain largely uncertain because of the limited availability of measurements, their clustered spatial distribution and their biased representativeness. For instance, out of the 63 available local studies used by Laruelle et al. (2010), about 2/3 are located in Europe or the US with only one value for fjord environments.

Here, we use the MARCATS segmentation in conjunction with a denser network of 161 local flux estimates to establish regionalized estuarine CO_2 fluxes (FCO_2), at the global scale. 93 local FCO_2 estimates are used and complemented by 68 additional FCO_2 values derived from estimates of the Net Ecosystem Metabolism (NEM) reported by Borges and Abril, 2011. For the latter, the linear FCO_2-NEM regression established by Maher and Eyre (2012) is used. The raw data are then clustered to derive a flux estimate for each estuarine type considered here (small deltas, tidal systems, lagoons, fjords). In MARCATS where at least two local studies are available for a given estuarine type (n=14, Fig 7a), the emission rate is directly extrapolated from the measurements and the total surface area of the estuarine type within the given MARCATS (Table 4). Their cumulative surface area amounts to 184 10^3 km^2, which corresponds to 17% of the world total for all types and 30% if only small deltas, tidal systems and lagoons are taken into account. For the other MARCATS

(n=31), the global area-specific average flux calculated for each type ($\overline{FCO_2}$, table 4) is used and multiplied by the type specific estuarine surface-area for the corresponding MARCATS.

Estuaries in Western Europe (IBE, NEA) are dominated by heavily polluted tidal systems and are hotspots of CO_2 emissions with average rates up to 28 mol C m^{-2} yr^{-1} (Fig 7b). European marginal seas, however, are characterized by lower values (BAL, MED). The region comprising the estuaries of India, Bangladesh and Indonesia (EAS, BEN, TEI) displays emission rates >20 mol C m^{-2} yr^{-1} but, because of a smaller estuarine surface area (table3), the total CO_2 evasion from Indian estuaries is substantially lower than that of Western Europe (6.5 vs 13.4 Tg C yr^{-1}), as also calculated by Sarma et al. (2012). The estuarine outgassing from the Western, Southern and Eastern coasts of the US (CAL, MEX, FLO) derived from local FCO_2 yields smaller values between 11.7 and 14.1 mol C m^{-2} yr^{-1}. Under warmer latitudes, BRA, TEA and TWI, exhibit emission rates >15 mol C m^{-2} yr^{-1} while the Eastern Australian coasts (EAC), displays the lowest rate of any region (3.0 mol C m^{-2} yr^{-1}). This average is largely influenced by the estuaries studied by Maher and Eyre (2012) which are characterized by an intake of atmospheric CO_2.

In MARCATS for which the number of available local FCO_2 per estuarine type is less than two, the average emission rate solely reflect the relative distribution in estuarine types. The regions where fjords dominate such as in the Northern parts of America and Europe (LAB, HUD, CAN, NGR, SGR, Fig 7b) are those where emission rates per unit surface area are the lowest (<10 mol C m^{-2} yr^{-1}). North Western Russia (BKS) and North Pacific (NEP, WEP) estuaries are characterized by a mix of fjords and tidal systems and their emission rates exceed 10 mol C m^{-2} yr^{-1}. In the rest of the world, the average emission rates are usually comprised between 15 and 18 mol C m^{-2} yr^{-1}.

Global average FCO_2 per unit surface area for small deltas, tidal systems, lagoons and fjords are 14.7, 18.2, 15.1 and 5.0 mol C m^{-2} yr^{-1}, respectively. The CO_2 emission

in the first three estuarine types is not significantly different from each other. However, they may vary markedly at the regional scale of MARCATS, for instance, by a factor of 6 in BEN where small deltas exhibit averages emission rates of 5.1 mol C m^{-2} yr^{-1} compared to 33.2 mol C m^{-2} yr^{-1} for lagoons. Other MARCATS where this regional difference is significant include IBE and NEA, where FCO_2 rates per surface area in tidal systems are twice higher than those of other systems. In SEA, on the other hand, small deltas'outgassing rate is as high as 41.8 mol C m^{-2} yr^{-1} compared to 18.9 mol C m^{-2} yr^{-1} for tidal systems. These differences support a regionalized analysis of estuarine CO_2 emissions.

Our calculations yield a global CO_2 evasion of 0.15 Pg C yr^{-1} for all estuaries. In order of decreasing importance, tidal systems, lagoons, fjords and small deltas contribute 0.063 Pg C yr^{-1}, 0.046 Pg C yr^{-1}, 0.025 Pg C $yr^{-1}$and 0.019 Pg C yr^{-1}, respectively. The global evasion estimates corresponds to an averaged emission rate per unit surface area of 13 mol C m^{-2} yr^{-1} which is higher than the mean rate of 6.9 mol C m^{-2} yr^{-1} proposed by Maher and Eyre (2012) but lower than previous estimates based on direct FCO_2 measurements (e.g. 21±18 mol C m^{-2} yr^{-1} for Laruelle et al., 2010), although still falling within the range of uncertainty. The smaller CO_2 evasion from fjords calculated here (5.1 mol C m^{-2} yr^{-1}, averaged over 7 values) largely explains most of the difference between our estimate and the one reported from a single measurement (17.5 mol C m^{-2} yr^{-1}) in Laruelle et al. (2010). Our analysis reveals that the spatial coverage of field data remains very coarse for accurate CO_2 flux estimations at the global scale, but the spatial resolution of the MARCATS units is well adapted to this scarcity and allows a first regionalized analysis.

Table 4: Air-water CO_2 fluxes for each estuarine type based on field studies. Positive values represent a source of CO_2 to the atmosphere. * indicates a CO_2 rate calculated from a NEM estimate and + indicates sites used to derive regional averages. Global emissions per unit surface area based on direct FCO_2 and derived from NEM lead to similar results for small deltas (14.6 molC m^{-2} yr^{-1} vs 15.2 molC m^{-2} yr^{-1}, average 14.7 molC m^{-2} yr^{-1}), lagoons (18.3 molC m^{-2} yr^{-1} vs 13.4 molC m^{-2} yr^{-1}, average 15.1 molC m^{-2} yr^{-1}) and fjords (5 molC m^{-2} yr^{-1} vs 4.9 molC m^{-2} yr^{-1}, average 5.0 molC m^{-2} yr^{-1}). In the case of tidal systems, direct FCO_2 (25 molC m^{-2} yr^{-1}) are ~ 2-3 times larger than NEM derived estimates (8.8 molC m^{-2} yr^{-1}) for an average of 18.2 molC m^{-2} yr^{-1}. This bias is likely due to the dominance of polluted European estuaries in the FCO_2 dataset while the NEM derived values are more homogeneously distributed (Maher and Eyre, 2012, Reville et al., 2002).

Site	*MARCATS*	*Long.*	*Lat.*	$\overline{FCO_2}$ *(molC m^{-2} yr^{-1})*	*Reference*
Small deltas					
Itacuraça creek (BR)	6	-44	-23	41.4	Borges et al. (2003)
Shark River (US)	9	-81.1	25.2	18.4	Koné and Borges (2008)
Duplin River (US) +	10	-81.3	31.5	21.4	Wang and Cai (2004)
Norman's Pond (BS) +	10	-76.1	23.8	5.0	Borges et al. (2003)
Rio San Pedro (ES)	19	-5.7	36.6	39.4	Ferrón et al. (2007)
Kidogoweni creek (KE) +	26	39.5	-4.4	23.7	Bouillon et al (2007a)
Mtoni (TZ) +	26	39.3	-6.9	7.3	Kristensen et al. (2008)
Ras Dege creek (TZ) +	26	39.5	-6.9	12.4	Bouillon et al. (2007c)
Matolo/Ndogwe/Kalota/Mto Tana (KE)	27	40.1	-2.1	25.8	Bouillon et al. (2007b)
Kali (IN) +	30	74.8	14.2	1.2	Sarma et al. (2012)
Mandovi (IN) +	30	73.8	15.4	6.6	Sarma et al. (2012)
Netravathi (IN) +	30	74.9	12.9	25.8	Sarma et al. (2012)
Sharavathi (IN) +	30	74.4	14.3	3.7	Sarma et al. (2012)
Zuari (IN) +	30	73.8	15.4	2.3	Sarma et al. (2012)
Ambalayaar (IN) +	31	79.5	10	0.0	Sarma et al. (2012)
Baitarani (IN) +	31	86.5	20.5	7.3	Sarma et al. (2012)
Cauvery (IN) +	31	79.8	11.4	0.8	Sarma et al. (2012)
Gaderu creek (IN) +	31	82.3	16.8	20.4	Borges et al. (2003)
Krishna (IN) +	31	81	16	2.5	Sarma et al. (2012)
Mooringanga creek (IN) +	31	89	22	8.5	Borges et al. (2003)
Nagavali (IN) +	31	84	18.2	0.1	Sarma et al. (2012)
Penna (IN) +	31	80	14.5	1.9	Sarma et al. (2012)
Rushikulya (IN) +	31	85	19.5	0.0	Sarma et al. (2012)
Saptamukhi cree (IN) +	31	89	22	20.7	Borges et al. (2003)
Vaigai (IN) +	31	79.8	10	0.1	Sarma et al. (2012)
Vamsadhara (IN) +	31	84.1	18.3	0.1	Sarma et al. (2012)
Vellar (IN) +	31	79	10	6.2	Sarma et al. (2012)
Khura river estuary (TH) +	32	98.3	9.2	35.7	Miyajima et al. (2009)
Trang river estuary (TH) +	32	99.4	7.2	30.9	Miyajima et al. (2009)
Nagada creek (ID)	37	145.8	-5.2	15.9	Borges et al. (2003)
Kiên Vàng creeks (VN) +	38	105.1	8.7	34.2	Koné and Borges (2008)
Tam Giang creeks (VN) +	38	105.2	8.8	49.3	Koné and Borges (2008)
Elkhorn Slough Azevedo (US) +	2	-121.8	36.8	15.2*	Caffrey (2004)
Elkhorn Slough South Marsh (US) +	2	-121.8	36.8	11.2*	Caffrey (2004)
South Slough Stengstacken (US) +	2	-124.3	43.3	14.5*	Caffrey (2004)
South Slough Winchester (US) +	2	-124.3	43.3	10.6*	Caffrey (2004)
Tijuana river Oneonta slough (MX) +	2	-117	32.5	23.7*	Caffrey (2004)
Tijuana river Tidal Linkage (MX) +	2	-117	32.5	24.7*	Caffrey (2004)
Tomales Bay (US) +	2	-122.9	38.1	6.3*	Smith and Hollibaugh (1997)
$\overline{FCO_2}$**, small deltas**			***avg.***	***14.7***	
Tidal systems					
Piauí River estuary (BR)	6	-37.5	-11.5	13.0	Souza et al. (2009)
Altamaha Sound (US) +	10	-81.3	31.3	32.4	Jiang et al. (2008)
Bellamy (US) +	10	-70.9	43.2	3.6	Hunt et al. (2010)
Cocheco (US) +	10	-70.9	43.2	3.1	Hunt et al. (2010)
Doboy Sound (US) +	10	-81.3	31.4	13.9	Jiang et al. (2008)
Great Bay (US) +	10	-70.9	43.1	3.6	Hunt et al. (2010)
Little Bay (US) +	10	-70.9	43.1	2.4	Hunt et al. (2010)
Oyster (US) +	10	-70.9	43.1	4.0	Hunt et al. (2010)

Parker River Estuary (US) +	10	-70.8	42.8	1.1	Raymond and Hopkinson
Sapelo Sound (US) +	10	-81.3	31.6	13.5	Jiang et al. (2008)
Satilla River (US) +	10	-81.5	31	42.5	Cai and Wang (1998)
York River (US) +	10	-76.4	37.2	6.2	Raymond et al. (2000)
Hudson River (Tidal) (US) +	10	-74	40.6	13.5	Raymond et al. (1997)
Florida Bay (US) +	10	-80.68	24.96	1.4	Dufore (2012) (Msc. Thesis)
Elbe (DE) +	17	8.8	53.9	53.0	Frankignoulle et al. (1998)
Ems (DE) +	17	6.9	53.4	67.3	Frankignoulle et al. (1998)
Rhine (NL) +	17	4.1	52	39.7	Frankignoulle et al. (1998)
Scheldt (BE/NL) +	17	3.5	51.4	63.0	Frankignoulle et al. (1998)
Thames (UK) +	17	0.9	51.5	73.6	Frankignoulle et al. (1998)
Douro (PT) +	19	-8.7	41.1	76.0	Frankignoulle et al. (1998)
Gironde (FR) +	19	-1.1	45.6	30.8	Frankignoulle et al. (1998)
Guadalquivir (ES) +	19	-6	37.4	31.1	de La Paz et al. (2007)
Loire (FR) +	19	-2.2	47.2	27.1	Bozec et al. (2012)
Sado (PT) +	19	-8.9	38.5	31.3	Frankignoulle et al. (1998)
Saja-Besaya (ES) +	19	-2.7	43.4	52.2	Ortega et al. (2004)
Tamar (UK) +	19	-4.2	50.4	74.8	Frankignoulle et al. (1998)
Betsiboka (MG)	26	46.3	-15.7	3.3	Ralison et al. (2008)
Tana (KE)	27	40.1	-2.1	47.9	Bouillon et al (2007b)
Bharatakulza +	30	75.9	10.8	4.3	Sarma et al. (2012)
Mandovi-Zuari (IN) +	30	73.5	15.3	14.2	Sarma et al. (2001)
Narmada (IN) +	30	72.8	21.7	3.2	Sarma et al. (2012)
Sabarmathi (IN) +	30	73	21	3.7	Sarma et al. (2012)
Sabarmathi (IN) +	30	73	21	5.1	Sarma et al. (2012)
Tapti (IN) +	30	72.8	21.2	132.3	Sarma et al. (2012)
Haldia Estuary (IN) +	31	88	22	4.5	Sarma et al. (2012)
Hooghly (IN) +	31	88	22	5.1	Mukhopadhyay et al. (2002)
Subarnalekha +	31	88.3	21.5	0.0	Sarma et al. (2012)
Godavari (IN) +	31	82.3	16.7	52.6	Sarma et al. (2011)
Camden Haven (Aus) +	35	152.83	-31.63	-5.0	Maher and Eyre (2012)
Hastings River (Aus) +	35	152.91	-31.4	-1.0	Maher and Eyre (2012)
Wallis lake (Aus) +	35	152.5	-32.18	-5.0	Maher and Eyre (2012)
Mekong (VN) +	38	106.5	10	30.8	Borges (unpublished)
Zhujiang (Pearl River) (CN) +	38	113.5	22.5	6.9	Guo et al. (2009)
Changjiang (Yantze) (CN)	39	120.5	31.5	24.9	Zhai et al. (2007)
Apex NY Bight (US) +	10	-73.2	40.1	8.4*	Garside and Malone (1978)
Chesapeake Bay Jug Bay (US) +	10	-76.0	37.0	30.9*	Caffrey (2004)
Chesapeake Bay Patuxent Park (US) +	10	-76.0	37.0	14.0*	Caffrey (2004)
Chesapeake Bay Goodwin Island (US) +	10	-76.0	37.0	2.0*	Caffrey (2004)
Chesapeake Bay Taskinas Creek (US) +	10	-76.0	37.0	2.4*	Caffrey (2004)
Delaware Bay Blackwater Landing (US) +	10	-75.2	39.1	17.4*	Caffrey (2004)
Delaware Bay Scotton Landing (US) +	10	-75.2	39.1	12.1*	Caffrey (2004)
Douro (PT) +	19	-8.7	41.1	15.1*	Azevedo et al. (2006)
Ems-Dollar (GE) +	17	6.9	53.4	10.1*	Van Es (1977)
Great Bay Great Bay Buoy (US) +	10	-70.9	43.1	5.4*	Caffrey (2004)
Great Bay Squamscott River (US) +	10	-70.9	43.1	7.3*	Caffrey (2004)
Hudson River Tivoli South (US) +	10	-74.0	40.7	12.1*	Caffrey (2004)
Mullica River Buoy 126 (US) +	10	75.8	39.8	4.8*	Caffrey (2004)
Mullica River Lower Bank (US) +	10	75.8	39.8	14.5*	Caffrey (2004)
Narragansett Bay Potters Cove (US) +	10	-71.6	41.6	12.6*	Caffrey (2004)
Narragansett Bay T-wharf (US) +	10	-71.6	41.6	11.2*	Caffrey (2004)
Newport River Estuary (US) +	10	-76.7	34.8	5.7*	Kenney et al. (1988)
North Carolina Masonboro Inlet (US) +	10	-77.2	34.3	15.0*	Caffrey (2004)
North Carolina Zeke's Island (US) +	10	-77.8	34.2	18.4*	Caffrey (2004)
North Inlet-Winyah Bay (US) +	10	-79.3	33.3	8.7*	Caffrey (2004)
Oosterschelde (NL) +	17	3.5	51.4	5.3*	Scholten et al. (1990)
Ria de Vigo (SP) +	19	-8.8	42.3	3.5*	Prego (1993)
Ria Formosa (PT) +	19	-7.9	37.0	2.5*	Santos et al. (2004)
San Francisco Bay, North Bay (US) +	2	-122.3	37.7	14.0*	Jassby et al. (1993)
San Francisco Bay, South Bay (US) +	2	-122.3	37.7	5.1*	Jassby et al. (1993)

Scheldt estuary (BE/NL) +	17	3.5	51.4	10.3*	Gazeau et al. (2005a)
Southampton water (UK) +	19	-1.4	50.9	9.5*	Collins (1978)
Urdaibai (SP) +	19	-2.7	43.4	-6.3*	Revilla et al. (2002)
Waquoit Bay Central Basin (US) +	10	-70.6	41.6	15.0*	Caffrey (2004)
Waquoit Bay Metoxit Point (US) +	10	-70.6	41.6	12.1*	Caffrey (2004)
Wells Head of Tide (US) +	10	-70.6	43.3	21.8*	Caffrey (2004)
Wells Inlet (US) +	10	-70.6	43.3	3.4*	Caffrey (2004)
$\overline{FCO_2}$, tidal systems			***avg.***	18.2	
Lagoons					
Brazos River (BR) +	9	-94.8	29.4	6.6	Zeng et al (2011)
Neuse River (US) +	10	-76.4	35.2	4.7	Crosswell et al. (2012)
Aveiro lagoon (PT)	19	-8.7	40.7	12.4	Borges and Frankignoulle (unpublished)
Albufer des Grau (SP)	20	4.2	40	-3.0	Obrador & Pretus (2012)
Aby lagoon (CI) +	23	-3.3	4.4	-3.9	Koné et al. (2009)
Ebrié lagoon (CI) +	23	-4.3	4.5	31.1	Koné et al. (2009)
Potou lagoon (CI) +	23	-3.8	4.6	40.9	Koné et al. (2009)
Tagba lagoon (CI) +	23	-5	4.4	18.4	Koné et al. (2009)
Tendo laggon (CI) +	23	-3.2	4.3	5.1	Koné et al. (2009)
Chalakudi (IN) +	30	76.3	10.2	4.7	Sarma et al. (2012)
Cochin (IN) +	30	76	9.5	55.1	Gupta et al. (2009)
Chilka (IN) +	31	85.5	19.1	31.2	Muduli et al. (2012)
Ponnayaar (IN) +	31	79.8	11.8	35.2	Sarma et al. (2012)
ACE Big Bay Creek (US) +	10	-80.3	32.5	30.9*	Caffrey (2004)
ACE St. Pierre (US) +	10	-80.4	32.5	17.4*	Caffrey (2004)
Apalachicola Bottom (US) +	9	-85.0	29.7	16.4*	Caffrey (2004)
Apalachicola Surface (US) +	9	-85.0	29.7	12.1*	Caffrey (2004)
Bojorquez Lagoon (MX)	8	-87	21.0	-17.6*	Reyes and Merino (1991)
Cochin (IN) +	30	76.0	9.5	6.3*	Gupta et al. (2009)
Copano Bay (US) +	9	-97.1	28.1	13.5*	Russell and Montagna (2007)
Estero Pargo (MX) +	9	-91.6	18.6	6.5*	Day et al. (1988)
Fourleague Bay (US) +	9	-91.2	29.3	8.8*	Randall and Day (1987)
Laguna Madre (US) +	9	-97.4	26.5	5.7*	Odum and Hoskin (1958), Odum and Wilson (1962), Ziegler and Benner (1998)
Lavaca Bay (US) +	9	-96.6	28.7	11.2*	Russell and Montagna (2007)
Mitla Lagoon (MX)	3	-96.4	16.9	13.1*	Mee (1977)
Nueces Bay (US) +	9	-97.4	27.3	-0.1*	Russell and Montagna (2007)
Ochlockonee Bay (US) +	9	-84.4	30.0	4.5*	Kaul and Froelich (1984)
Redfish Bay (US) +	9	-97.1	27.9	20.2*	Odum and Hoskin (1958)
Rookery Bay Blackwater River (US) +	9	-81.4	26.0	41.1*	Caffrey (2004)
Rookery Bay Upper Henderson (US) +	9	-81.4	26.0	33.4*	Caffrey (2004)
San Antonio Bay (US) +	9	-96.7	28.3	9.8*	Russell and Montagna (2007)
Sapelo Flume Dock (US) +	10	-81.2	31.5	22.3*	Caffrey (2004)
Sapelo Marsh Landing (US) +	10	-81.2	31.5	13.6*	Caffrey (2004)
Saquarema Lagoon (BR)	6	-42.5	-22.9	3.9*	Carmouze et al. (1991)
Terminos lagoon (MX) +	9	-91.6	18.6	4.4*	Day et al. (1988)
Venice Lagoon (IT)	20	12.3	45.4	51.0*	Ciavatta et al. (2008)
Weeks Bay Fish River (US) +	9	-87.8	30.4	2.9*	Caffrey (2004)
Weeks Bay Weeks Bay (US) +	9	-87.8	30.4	4.8*	Caffrey (2004)
$\overline{FCO_2}$, lagoons			***avg.***	15.1	
Fjords					
Bothnian Bay (FI) +	18	21	63	3.1	Algesten et al. (2004)
Godthåbsfjord (GR)	15	-51.7	64	-7.95	Rysgaard et al. (2012)
Liminganlahti Bay (FI) +	18	25.4	64.9	7.5	Silvennoinen et al. (2008)
Randers Fjord (DK) +	18	10.3	56.6	17.5	Gazeau et al. (2005)
Nordasvannet Fjord (NO)	17	5.3	60.3	3.8*	Wassmann et al. (1986)
Padilla Bay Bay View (US)	2	-122.5	48.5	5.8*	Caffrey (2004)
Randers Fjord (DK)	18	10.3	56.6	4.9*	Gazeau et al. (2005b)
$\overline{FCO_2}$, fjords			***avg.***	5.0	

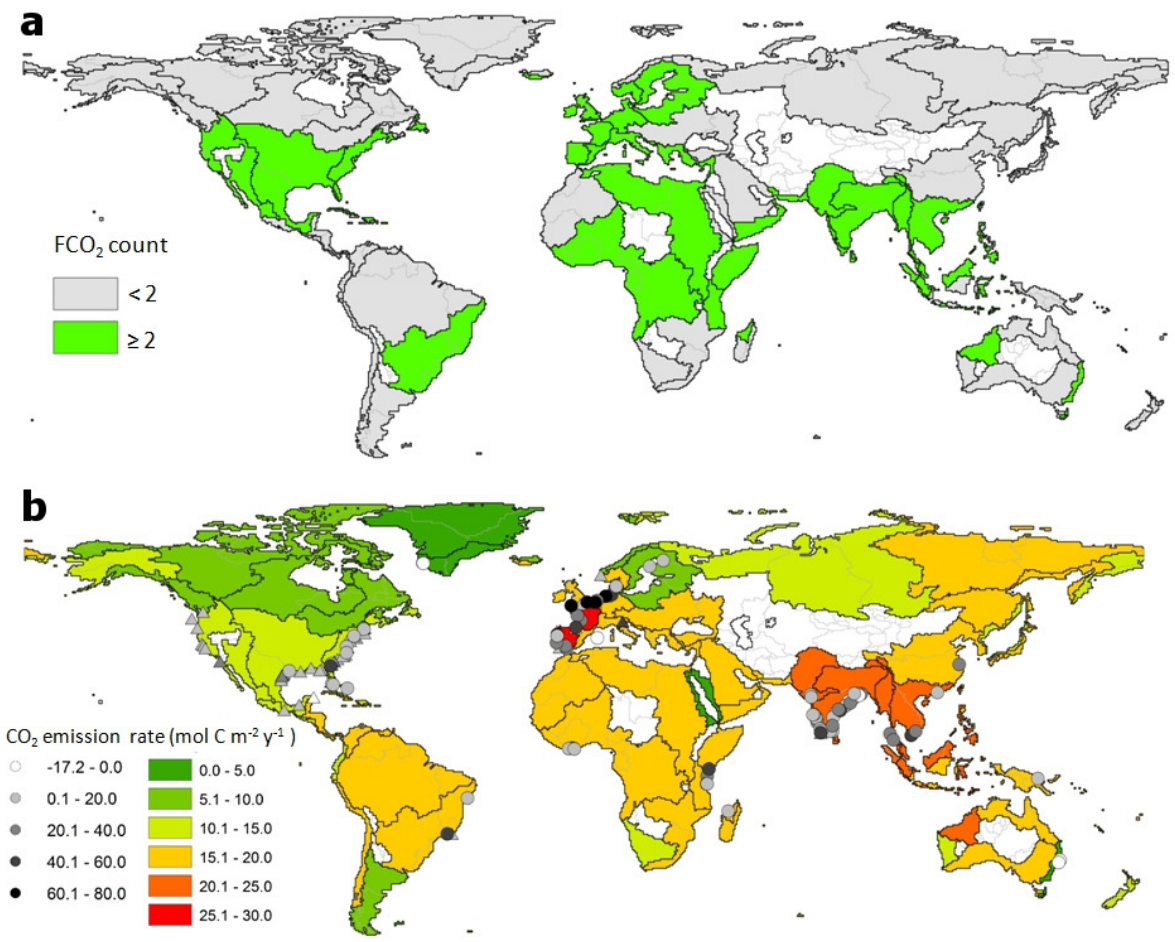

Figure 1: (a) Number of local air-water CO_2 flux estimates available per MARCATS (black lines), COSCATs limits are indicated by grey lines. (b) Air-water CO_2 emission rates for estuaries from direct estimates (dots) and derived from Net Ecosystem Metabolism (triangles). Mean rates per MARCATS are represented by the color scale.

4. Conclusions and Outlook

In this study, a three level segmentation of the land-ocean continuum extending from the watersheds to the shelf break has been proposed. The 0.5 degrees resolution of our level I compares to the highest resolution available for most global hydrological models and watershed GIS models. At this resolution, the routing amongst the vast majority of river networks is properly represented and terrestrial GIS models are able to produce reliable riverine discharge estimates for large and medium sized rivers (watersheds> ten terrestrial cells, Beusen et al., 2005). In addition, important terrestrial and coastal global databases cluster information at the same resolution of 0.5 – 1 degree (e.g. World Ocean Atlas, Da Silva, 1994, Hexacoral), making combination and meta-analysis between data sets relatively easy. Recent coastal analyses (LOICZ, Buddemeier et al., 2008, Crossland et al., 2005) and typologies (Dürr et al., 2011) as well as GIS models such as the GLOBALNEWS initiative (Mayorga et al., 2010, Seitzinger et al., 1995) have also been developed at 0.5-1°. However, with the exception of a few areas around the world (e.g. COSCAT 827 along the east coast of the US; Regnier et al., Submitted), the network of biogeochemically relevant observations of the aquatic continuum is not dense enough at this resolution and calls for an analysis at a coarser resolution.

Levels II and III are used to construct large regional entities which retain the most important climatic, morphological and hydrological characteristics of continental waters and the coastal ocean. The resulting number of segments (149 COSCATs and 45 MARCATS) can easily be manipulated and compared to existing segmentations such as the LME (Sherman et al., 1998) or that of Seiter et al. (2005). The segments provide globally consistent estimates of hypsometric profiles, surface areas and volumes that can be used in combination with databases to establish regional and global biogeochemical budgets. In addition, the inter-compatibility between the three levels allows combining databases compiled at different

spatial scales. Here, the segmentation is used to establish regionalized estuarine CO_2 flux through the air-water interface. As data are progressively building up, the procedure could easily be extended to inland waters and the coastal ocean. The spatially resolved representation of the hydrological cycle from the river network to the coastal ocean allows also for a quantitative treatment of the water flow routing through the different estuarine types. Both freshwater flow and CO_2 budgets are performed at the scale of the MARCATS. In the future, our calculation could also address lateral fluxes of terrestrial carbon, nutrients and further elements being relevant in Earth system science. The multi-scale segmentation of the aquatic continuum from land to ocean thus provides an appropriate support for an optimal use of global biogeochemical databases (Cai, 2011, Chen et al., 2012, Crossland et al., 2005, Gordon et al, 1996, Laruelle et al., 2010, Nixon et al, 1996) and will allow to construct increasingly robust regionalized budgets of relevance to environmental and climate research.